Soft Matter

Accepted Manuscript

ROYAL SOCIETY OF CHEMISTRY

www.rsc.org/softmatter

Soft Matter

RSCPublishing

PAPER

From coffee rings to coffee eyes†

Cite this: DOI: 10.1039/x0xx00000x

Yanshen Li,[a,b] Cunjing Lv,[a,b,c] Zhaohan Li,[a] David Quéré,*[c] Quanshui Zheng*[a,b]

Received 00th January 2015
Accepted 00th January 2015

DOI: 10.1039/x0xx00000x

www.rsc.org/

We discuss how the stain left after evaporation of a suspension evolves as heating glass or plastic on which the liquid has been deposited. As increasing the substrate temperature, it is found that the stain gradually changes from the usually observed ring to an "eye", that is, a combination of thick central stain and thin outer ring. Both the size and relative volume of the central stain increase with the substrate temperature. The main mechanism for this phenomenon is proposed to be an enhanced Marangoni recirculation flow on hot substrat These findings can be exploited to continuously tune the morphology of coffee stains, with potential applications in self-assembly and ink-jet printing.

Introduction

A sessile droplet containing dispersed insoluble particles forms a ring after its evaporation in ambient condition. This so-called "coffee ring" effect[1, 2] has been intensively studied due to its wide applications in fabrication of micro-arrays[3, 4] or devices,[5, 6] coatings,[7-10] ink-jet printing,[11-13] biosensors[14, 15] and particles self-assembly.[16] It has been established that coffee rings appear on two main conditions:[1] (1) a faster evaporation near the solid-liquid-vapour contact line than in the central liquid-vapour interfacial area; (2) a pinning of the contact line during most (or even all) of the evaporation process. These conditions lead to the onset of an outward radial flow from the bulk to the edge, which continuously feeds the contact line with particles as liquid evaporates, until leaving an annular stain.

Other morphologies for the final deposit also attracted attention. It was found that minimizing contact angle hysteresis can lead to the formation of a central stain, rather than a ring.[17-19] Particles that spontaneously adsorb at the substrate[20] or migrate at the liquid-vapour interface[21] also oppose the coffee ring effect. Even in the presence of pinning, the ring formation can be impeded by the presence of a reverse (i.e. inward) flow during evaporation,[22, 23] which can be caused by temperature-driven or surfactant-induced Marangoni effect.[24, 25]

We discuss here how heating the substrate can modify the stain. In a phenomenon where evaporation plays a major role, the substrate temperature is a natural parameter that should influence the kinetics of the process and possibly the pattern of the ring, which, to our knowledge, was surprisingly not considered in the literature. We report that "eye-like stains" appear when drying colloidal drops on heated substrates of low thermal conductivity.

[a] *Department of Engineering Mechanics and* [b] *Center for Nano and Micro Mechanics, Tsinghua University, Beijing 100084, China. E-mail: zhengqs@tsinghua.edu.cn*

[c] *Physique et Mécanique des Milieux Hétérogènes, UMR 7636 du CNRS, ESPCI, 75005 Paris, France. E-mail: david.quere@espci.fr*

† Supplementary Information (SI) available: experimental details, supporting discussions and movies. See DOI: 10.1039/b000000x/

Experimental setup & results

Water drops with uniformly dispersed polystyrene (PS) spheres of diameter ~100 nm and concentration 2.5 mg/mL are deposited on a glass slide itself placed on an electronic heater. If not specified, the initial volume of drops is 2.5 ± 0.1 µL. Experiments are carried out in ambient air, and air temperature and relative humidity are fixed to 24 ± 1°C and 55 ± 1%. The substrate is first ultrasonically cleaned in isopropanol for 15 minutes, then in de-ionized water for another 15 minutes, and dried with compressed dry nitrogen. Probing a randomly picked area of 100 µm × 100 µm by an atomic force microscope (AFM) (NTEGRA Aura, NT-MDT, Russia) in tapping mode provides a RMS roughness of 3.4 nm. Advancing and receding contact angles of water on the cleaned substrate are measured and found to be 49.1 ± 1.5° and 6.6 ± 2.4°, respectively. The corresponding angle hysteresis is large enough to pin the drop edges, so that the diameter of the stain left after evaporation (3.5-4 mm) is the same as the initial diameter of the drop. The substrate temperature T is controlled and kept constant during each experiment at preset values ranging from 30 to 80°C. For each experiment, the temperature of the substrate is measured with a resistance thermal detector (RTD) Pt100 (PTFN, Sensotherm, Germany) of size 5mm × 1.6mm × 1.1mm. Once stabilized, temperature is recorded at the corners of the substrate and at its centre, at a distance of 4mm from drops' edges: its variation within the heated area is found to be ±1°C (see Supplemental Information for more details about the samples and temperature measurements †).

White light interferometry (AEP Technology, USA) was chosen to determine the 3D-configuration of the stain pattern. Stains are coated in a vacuum evaporation chamber with a 7~8 nm-thick Pt layer. White light interferometry makes use of two waves of same frequency, and the resulting interference figure provides the profile of the stain. This technique widely studied [26-30] has a remarkable precision, down to 0.1 nm in the z-direction.

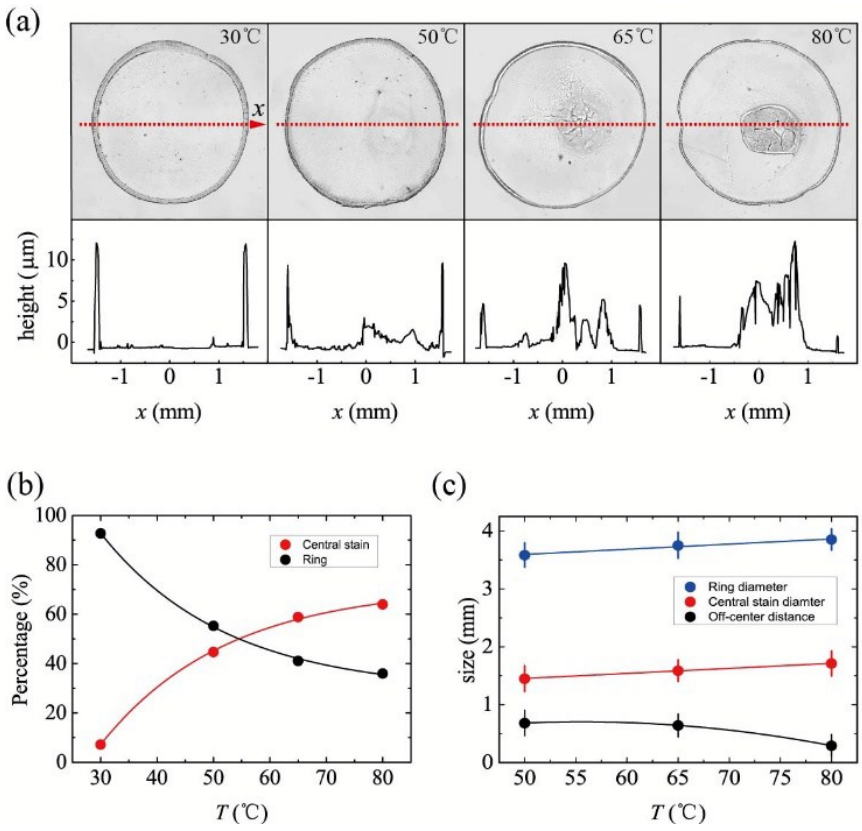

Figure 1. Final stain after evaporation of a suspension, as a function of the substrate temperature T. (a) First and second rows show top view and corresponding cross-sections measured by interferometry along the red lines. Temperature of the glass substrate is 30, 50, 65 and 80°C. Droplets, of initial volume 2.5 µL, are made of water containing 2.5 mg/mL of 100 nm-PS spheres. A central stain gradually appears as increasing the substrate temperature T, and the ring consequently thins. (b) Proportion of particles in the central stain (red), as deduced from cross-section profiles, and proportion of particles in the ring (black). (c) Diameter (red) and center position (black) of the central stain, and diameter of the ring (blue) as functions of T. Each point is an average on 20 experiments, and bars indicate the standard deviation of data.

Soft Matter RSCPublishing

PAPER

Figure 1 shows how the pattern adopted by the particles after evaporation depends on the substrate temperature. We display in Figure 1a a top view of the pattern together with its profile provided by interferometry. While a single ring (of typical height 12.0 ± 1.0 µm and width 0.10 ± 0.01 mm) is observed at $T = 30°C$, a combination of central stain and thinner ring appears as increasing the substrate temperature. At $T = 50°C$, for instance, the central stain has a height of 1.9 µm and width of 1.6 mm. As shown in Figure 1b, the relative volume of the central stain can be extracted from the profiles, which makes clear the continuous growth of this stain with T. The central deposit is often slightly off-centred, a consequence of the liquid reorganisation after the asymmetric breaking of the film. Figure 1c gives a statistics of its diameter and centre location: each point is an average on 20 experiments, and the bar indicates the standard deviation of data. These results confirm the increase of size of the central stain with T, and also exhibit a slight decrease of off-centring, a natural consequence of the weaker mobility of larger stains.

Interpretation

The flow in an evaporating sessile droplet can be more complex than just a radial motion. On substrates warmer than the surrounding atmosphere, the surface temperature of the droplet should decrease as going away from contact line, which generates a temperature gradient along the liquid-vapour interface. The corresponding gradient in surface tension induces an inward Marangoni flow from the hot region (the drop periphery) toward the cool one (the drop apex). [22, 24, 31-35] When the heat conductivity of the substrate compares to that of the liquid, recent models[36] and experiments[37] have shown that the maximum surface temperature is not at the contact line, but close to it: a higher evaporation rate at the line causes larger cooling effects despite smaller thermal resistance. This generates a shift of maximum temperature from the line to an inner stagnation point, [32, 34, 36] above which the liquid surface is entrained toward the apex of the drop (Figure 2a).

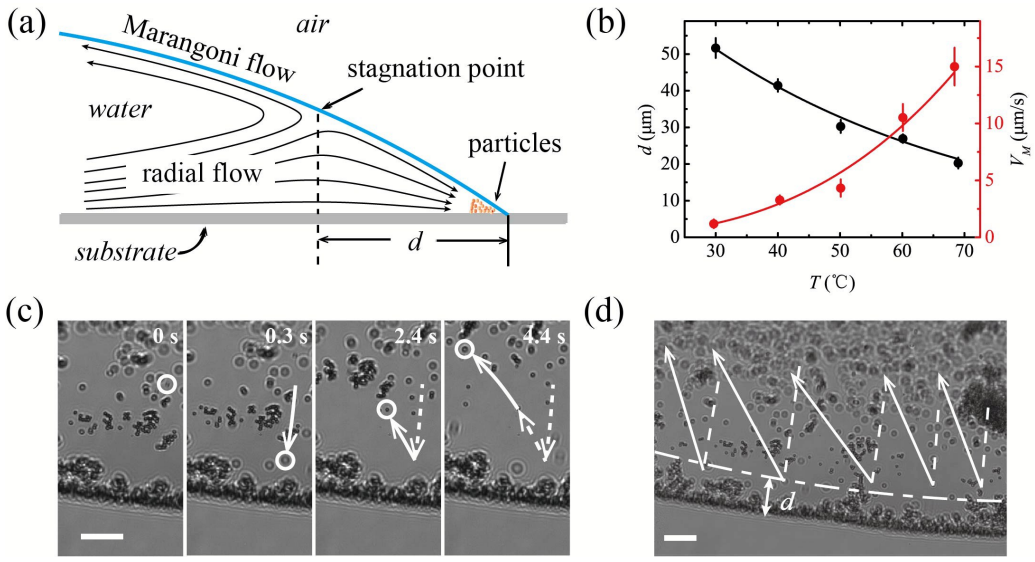

Figure 2. Flow field in an evaporating drop close to the contact line. (a) Sketch of the flow, made of an outward radial flow along the substrate (accumulating particles at the line) and an inward Marangoni flow along the liquid-vapor interface, which produces a stagnation point at a distance d to the line. (b) Measured distance d and surface flow velocity V_M as a function of the substrate temperature T. The velocity V_M is measured at 0.5 mm from the contact line. d is averaged over 5 experiments and V_M is averaged over 3 experiments. Error bars indicate standard deviations of the data. (c) Snapshots pointing out the successive positions of one particle located close to the drop surface. The tracer bounces back as it approaches the contact line. The bar indicates 20 µm. (d) Capture of five such trajectories. The distance between the (dotted) stagnation and (black) contact lines is the stagnation distance d. The bar indicates 20 µm.

In order to evidence the surface flow, we used an optical microscope (BX51, Olympus, Japan) connected to a CCD camera (Fastcam SA3, Photron, USA), and observed water droplets with large (1 μm) and dilute (0.25 mg/mL) dispersed polystyrene (PS) spheres. Figure 2c presents four frames selected from movie 1-2 (see SI†) showing the position of a PS sphere (circled in the figure) at 0, 0.3, 2.4 and 4.4s, for $T = 30°C$. The particle first moves toward the contact line before reversing its direction, confirming the existence of two opposite flows separated by a stagnation line. Focusing on the stagnation line, the focus of the microscope must be risen to keep track of the backward moving particles. This implies that backward particles are entrained along the droplet free surface, in agreement with the nature of a Marangoni flow. By using this method, we could identify the stagnation line, whose position is reported with a dotted line in Figure 2d. The distance d between stagnation and contact lines is typically 50 µm at $T = 30°C$ and it decreases with the substrate temperature T, as shown in Figure 2b. In the same plot, we also report typical surface velocities V_M "far" (at a fixed distance of 0.5 mm) from the contact line, measured by following the motion of polystyrene spheres under microscope. V_M increases with T, which suggests that Marangoni flows in the evaporating drop are enhanced on hotter substrates.

To understand in more details the impact of the inward flow on the final stain, we observe the whole drying at the drop scale for both low and high substrate temperatures. Drops are illuminated from aside, so that pure water surface is mostly dark due to mirror reflection. In contrast, particles at the surface scatter the incident light and turn into white (see SI Fig. S3†). Time 0 corresponds to the contact of the drop, which first spreads on the substrate in 2 to 4 s. Spreading stage is always much shorter than evaporation, which allows us to ignore the effect of this initial flow. Figure 3a shows six snapshots selected from movie 3 (see SI†), for a substrate at $T = 30°C$. The whole drying process lasts 488 seconds and it can be divided into three stages. In the first stage (0 – 337 s), the ring gradually builds up, as the result of the strong evaporation-driven radial flow opposed by a relatively weak inward surface flow. As time goes on, the contact angle decreases and the film flattens (so that the temperature becomes homogeneous), which both enhance the radial flow and makes the Marangoni flow vanish at the surface: this defines phase II (337 – 471 s). In the third, final stage (471 – 488 s), the thin flat remaining film cracks, retracts and evaporates, leaving only a few particles behind owing to its small volume. The film always breaks close to the ring, whose porous structure sucks liquid, so that local thinning (accelerated by evaporation) takes place in the ring vicinity and leads to this localized crack.

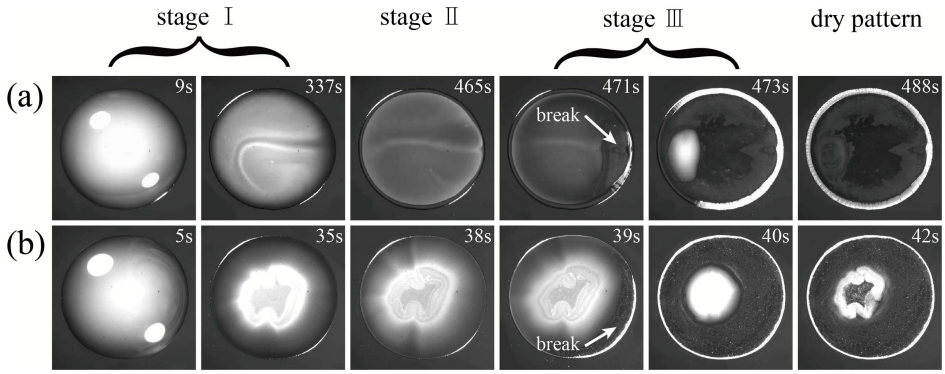

Figure 3. Evaporation of a 2.5 µL water droplet containing 2.5 mg/mL of 100 nm diameter PS spheres. Images are taken under microscope, with white light illuminating from aside. (a & b) correspond to substrate temperature of 30 and 70°C, respectively. In Stage I, inward and outward flows coexist and concentrate the particles: an evaporation-driven outward flow, dominant in a, and a surface temperature-driven inward flow, dominant in b. These flows respectively lead to the formation of an outward ring or of an inward island. In Stage II, the film becomes flat and thin, so that the surface Marangoni flow vanishes, leaving only the outward flow. In Stage III, the thin film of water breaks close to the ring and disappears, which fixes the final pattern of the stain.

Drying on hot substrates can be decomposed similarly, but phases I and II are quite different. Figure 3b and movie 4 (see SI†) show evaporation on a substrate at $T = 70°C$. Drying takes place in only 42 seconds, that is, about 10 times quicker than at $T = 30°C$. In the first stage (0 – 35 s), a much stronger Marangoni flow efficiently brings inward a large amount of particles that accumulate at the centre of the drop and constitute a central island. Contrasting with low temperature, the ring formation is marginal in this phase, confirming the dominant role of the inward surface flow. In phase II (35 – 39 s), the drop around the island becomes flat, which switches off Marangoni effects and makes the outward flow dominant: the island remains unchanged while a thin ring builds at the drop periphery (movie 4). The third stage (39 – 42 s) starts when the film cracks (again close to the line), which disconnects the island from the ring. The island itself dries, which leads to a partial reorganization of the particles and to the formation of a thick ring around it.

Discussion

Temperature differences generate Marangoni flows, but they could also drive a buoyant motion from the hot solid surface to the cooler apex of the drop. Let us compare the characteristics velocities V_M and V_B of these two flows. On the one hand, for a Marangoni flow and denoting $\beta = (\partial\gamma/\partial T)$ the variation of surface tension γ with temperature T, we can balance the tangential stress $\partial\gamma/\partial x \sim \beta\Delta T/R$ arising from surface tension gradients at the scale R of the droplet with the viscous stress $\eta V_M/h$, where η is the liquid viscosity and h a typical liquid thickness. Hence we get a Marangoni velocity V_M scaling as $\beta\Delta T h/\eta R$. On the other hand, for a liquid of contact angle θ and thermal expansion $\alpha = (\partial\rho/\partial T)$, the balance of buoyancy $\alpha\Delta T g h\theta$ with viscous stress $\eta V_B/h$ yields a buoyancy velocity V_B scaling as $\alpha\Delta T g h^2\theta/\eta$. Interestingly, the ratio V_M/V_B is independent of the (unknown) temperature difference ΔT, and found to scale as $\beta/(\alpha g h R\theta)$, a quantity on the order of 10 at the beginning of evaporation and increasing later (because h and θ then decrease), always much larger than unity: at the scale of a drop, Marangoni flows should generally dominate gravity-driven flows of same physical origin. This can be confirmed by turning upside down the experimental platform at $T = 80°C$, keeping unchanged other parameters. After evaporation, the stain left by a suspension (2.5 mg/mL) of dispersed PS spheres of diameter 100 nm is found similar to the one left in normal gravity.

In order to test the universality of the "coffee eye" phenomenon, we carried out series of experiments on substrates of various thickness and thermal conductivity: glass (0.2mm, 1mm or 3mm thick), polystyrene (1mm thick) and PMMA (5mm thick) of respective conductivity 0.85 W/mK, 0.3 W/mK and 0.2 W/mK all comparable to that of water (0.6 W/mK). Polysterene and PMMA are less hydrophilic than glass with measured advancing and receding angles of 94±1° and 39±3°, and 86±1° and 47±3°. These large hysteresis might arise from the significant RMS roughness found by AFM to be 20 nm and 12 nm, respectively. Despite the differences between substrates, eye stains appear on all of them heated at 70°C, without significant modification from the last image of Figure 1a (see SI Fig. S4†). In contrast, we only observe simple rings on aluminium, copper and silicon (between 30 and 80°C), of thermal conductivity 100 to 1000 higher. Following tracers under microscope, we see that there is indeed no inward flow in these situations. A conductive solid may erase temperature fluctuations in the liquid, and thus maximize edge evaporation and minimize Marangoni transport. This experiment anyway confirms the correlation between the existence of inward flows and the formation of central stains.

We can finally look at the influence of size and charge of the particles (see SI Fig. S5†). (i) Droplets with 1 μm diameter particles at a concentration of 2.5 mg/mL (same concentration as for smaller particles) on glass at $T = 70°C$ generate an eye stain comparable (yet slightly larger) to what was found earlier. (ii) PS colloids in water are charged, which explains the stability of the dispersion. This might be due to end groups[38] or to the use of potassium persulphate as an initiator of polymerization[39]. We tested the influence of charged additives by dissolving KOH (0.01M) in a solution (2.5 mg/mL) of 100nm-particles. Drops then dry in a similar manner: particles caught at the surface concentrate inward, which leads to a large eye-pattern (see SI Fig. S5b†), with a central bright spot believed to be KOH left at the end of the evaporation process. According to Bhardwaj,[40] the presence of potassium hydroxide increases the charge of the particles, which strengthens the repulsive force between particles and might participate to the formation of larger central stains.

Conclusions

We investigated the effect of substrate temperature on the morphology of coffee stains left after evaporation of aqueous suspensions. On substrates of low thermal conductivity (such as glass and polystyrene) hotter than ambient temperature ($T > 40°C$), we found that the well-known ring pattern drastically changes into an eye pattern,

that is, a combination of large central dot and thin ring. This pattern builds due to an efficient inward flow at the surface, which was interpreted as a Marangoni flow arising from temperature differences between drop edge and apex. This flow builds an island of particles at the drop centre and it impedes the formation of a ring, until the liquid film becomes flat enough to extinguish Marangoni effects, allowing a thin ring to form. This phenomenon can be exploited for tuning the shape of the pattern left after evaporation of a suspension such as ink: increasing the substrate temperature leads to a more homogeneous deposition, a situation of obvious interest if one looks at a regular appearance for ink spots. Conversely, these findings suggest that in model experiments where we try to accelerate aging processes (here, drying) by tuning a parameter (here, temperature), we can modify the physics of the underlying phenomena, and generate patterns that are not observed following a slower route. It would finally be interesting to study how a drop dries on a substrate with a gradient of temperature, which might help to control even further the design of the remaining stain.

Acknowledgements

Financial support from the NSFC under grant Nos. 11372153 and 11172149 is gratefully acknowledged and discussions with Bernard Cabane, Shuai Wu and Nan Xue were greatly appreciated.

Notes and references

1 R.D. Deegan, O. Bakajin, T.F. Dupont, G. Huber, S.R. Nagel and T.A. Witten, *Nature*, 1997, **389**, 827-829.
2 R.D. Deegan, *Phys. Rev. E*, 2000, **61**, 475-485.
3 M.C. Pirrung, *Angew. Chem. Int. Ed.*, 2002, **41**, 1276-1289.
4 M. Schena, D. Shalon, R. Heller, A. Chai, P.O. Brown and R.W. Davis, *Proc. Nat. Acad. Sci.*, 1996, **93**, 10614 -10619.
5 T. Kawase, H. Sirringhaus, R.H. Friend and T. Shimoda, *Adv. Mater.*, 2001, **13**, 1601-1605.
6 D.J. Norris, E.G. Arlinghaus, L. Meng, R. Heiny and L.E. Scriven, *Adv. Mater.*, 2004, **16**, 1393-1399.
7 N. Chakrapani, B. Wei, A. Carrillo, P.M. Ajayan and R.S. Kane, *Proc. Nat. Acad. Sci.*, 2004, **101**, 4009-4012.
8 B.J. de Gans, P.C. Duineveld and U.S. Schubert, *Adv. Mater.*, 2004, **16**, 203-213.
9 M. Kimura, M.J. Misner, T. Xu, S.H. Kim and T.P. Russell, *Langmuir*, 2003, **19**, 9910-9913.
10 J.N. Cawse, D. Olson, B.J. Chisholm, M. Brennan, T. Sun, W. Flanagan, J. Akhave, A. Mehrabi and D. Saunders, *Prog. Org. Coat.*, 2003, **47**, 128-135.
11 T. Kawase, T. Shimoda, C. Newsome, H. Sirringhaus and R.H. Friend, *Thin Solid Films*, 2003, **438**, 279-287.
12 D. Huang, F. Liao, S. Molesa, D. Redinger and V. Subramanian, *J. Electrochem. Soc.*, 2003, **150**, G412 -G417.
13 D. Soltman and V. Subramanian, *Langmuir*, 2008, **24**, 2224-2231.
14 J.T. Wen, C. Ho and P.B. Lillehoj, *Langmuir*, 2013, **29**, 8440-8446.
15 K. Sefiane, *J. Bionic Eng.*, 2010, **7**, S82-S93.
16 Y. Cai and B.M. Zhang Newby, *J. Am. Chem. Soc.*, 2008, **130**, 6076-6077.
17 H.B. Eral, D.M. Augustine, M.H.G. Duits and F. Mugele, *Soft Matter*, 2011, **7**, 4954-4958.
18 A. Lafuma and D. Quere, *EPL*, 2011, **96**, 56001.
19 Y. Li, Y. Sheng and H. Tsao, *Langmuir*, 2013, **29**, 7802-7811.
20 A. Crivoi and F. Duan, *Langmuir*, 2013, **29**, 12067-12074.
21 P.J. Yunker, T. Still, M.A. Lohr and A.G. Yodh, *Nature*, 2011, **476**, 308-311.
22 H. Hu and R.G. Larson, *Langmuir*, 2005, **21**, 3972-3980.
23 B.M. Weon and J.H. Je, *Phys. Rev. Lett.*, 2013, **110**, 028303.
24 H. Hu and R. G. Larson, *J. Phys. Chem. B*, 2006, **110**, 7090-7094.
25 T. Still, P.J. Yunker and A.G. Yodh, *Langmuir*, 2012, **28**, 4984-4988.
26 E.N. Leith and G.J. Swanson, *Appl. Opt.*, 1980, **19**, 638-644.
27 Y. Cheng and E.N. Leith, *Appl. Opt.*, 1984, **23**, 4029-4033.
28 E.N. Leith and R. Hershey, *Appl. Opt.*, 1985, **24**, 237-239.
29 J.C. Wyant, *Proceedings of the SPIE*, 2002, **4737**, 98-107.
30 Y. Wyart, R. Tamime, L. Siozade, I. Baudin, K. Glucina, C. Deumié and P. Moulin, *J. Membr. Sci.*, 2014, **472**, 241-250.
31 J.R. Trantum, Z.E. Eagleton, C.A. Patil, J.M. Tucker-Schwartz, M.L. Baglia, M.C. Skala and F.R. Haselton, *Langmuir*, 2013, **29**, 6221-6231.
32 G. Fabien, M. Antoni and K. Sefiane, *Langmuir*, 2011, **27**, 6744-6752.
33 X. Xu, J. Luo and D. Guo, *Langmuir*, 2009, **26**, 1918-1922.
34 X. Xu, J. Luo and D. Guo, *Soft Matter*, 2012, **8**, 5797-5803.
35 W.D. Ristenpart, P.G. Kim, C. Domingues, J. Wan and H.A. Stone, *Phys. Rev. Lett.*, 2007, **99**, 234502.
36 L. Ma, X. Xu, J. Luo, D. Guo and K. Zhang, *Phys. Rev. E*, 2014, **89**, 032404.
37 X. Xu and J. Luo, *Appl. Phys. Lett.*, 2007, **91**, 124102.
38 K. Roger, M. Eissa, A. Elaissari and B. Cabane, *Langmuir*, 2013, **29**, 11244-11250.
39 A. Kotera, K. Furusaw and Y. Takeda, *Kolloid-Zeitschrift und Zeitschrift für Polymere,* 1970, **239**, 677-681.
40 R. Bhardwaj, X. Fang, P. Somasundaran and D. Attinger, *Langmuir*, 2010, **26**, 7833-7842.

TOC

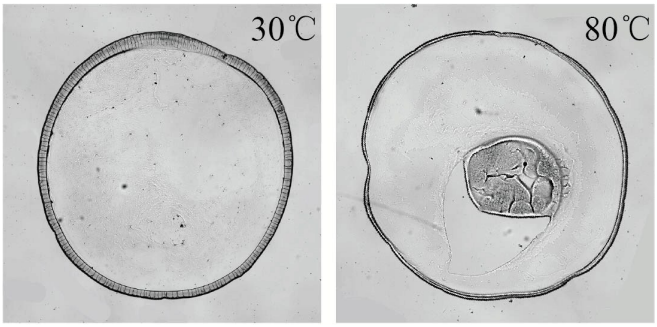

The morphology of the deposit after evaporation of a suspension changes from a ring shape to an eye shape, that is, a combination of central stain and thinner ring, when increasing the substrate temperature.